Asociación Argentina
de Mecánica Computacional

Mecánica Computacional Vol XXIX, págs. 7557-7569 (artículo completo)
Eduardo Dvorkin, Marcela Goldschmit, Mario Storti (Eds.)
Buenos Aires, Argentina, 15-18 Noviembre 2010

ANALYTICAL AND NUMERICAL TOOLS FOR BONDED JOINT ANALYSIS

René Q. Rodríguez[a], William P. Paiva[a], Paulo Sollero[a], Eder L. Albuquerque[b] and Marcelo B. Rodrigues[c]

[a] *Universidade Estadual de Campinas, Rua Mendeleyev, 200, Cidade Universitária "Zeferino Vaz", Campinas, Brasil, sollero@fem.unicamp.br*

[b] *Universidade de Brasília, Campus Universitário "Darcy Ribeiro", Brasília, Brasil, eder@unb.br*

[c] *Empresa Aeronáutica Brasileira, Avenida Brigadeiro Faria Lima, 2170, São José dos Campos, Brasil, marcelo.bertoni@embraer.com.br*

Keywords: adhesively bonded joints, analytical methods, failure criteria, stress distribution, software implementation.

Abstract. Application of adhesives in bonded joints is increasing. Therefore, there is a specific need for analysis and design tools that can provide physical insight and accurate results for bonded joints applications. These tools would be very useful for preliminary design purposes, which would reduce costly tests. Several analytical methods for calculations of stress distributions in adhesively bonded joints are available in literature. However, implementation and use of analytic models are usually difficult, since they are complex non-linear functions of material properties and geometry. This paper presents a Matlab® implementation of analytic solutions in a user-friendly software. Software permits calculation of stress distributions using each analytical solution individually, comparisons among different analytic solutions results and failure criteria analysis. The ABAQUS®, a commercial finite element software, was used for the numerical validation. For the experimental validation, predicted strengths were compared with test data obtained by several tests performed according to the American Society for Testing and Materials (ASTM). Finally a failure criterion was implemented.

1 INTRODUCTION

Development of new materials and processes is followed by considerable advances in structural design. Optimized design of structures frequently requires the usage of dissimilar materials together. Sometimes materials cannot be welded, in other cases structures do not admit bolted or riveted connections. As an alternative, application of adhesives in bonded joints is increasing. Therefore, there is a specific need for analysis and design tools that can provide physical insight and accurate results for bonded joints applications. This paper presents the development of an interactive tool for analysis of stress distribution in adhesively bonded joints. Initially, it is shown a review of the main analytical methods found in literature. Further, the implementation of the software is described. Finally, implemented models are validated by comparing its result against numerical and experimental results. Numerical results were obtained by using the commercial finite element software ABAQUS. Experimental results were obtained from tests carried according to the American Society for Testing and Materials (ASTM).

2 ANALYTICAL MODELS

2.1 Volkersen

The first analytical method known in literature for the stress analysis of bonded joints was developed by Volkersen (1938). Volkersen method, also known as the "shear-lag model", introduced the concept of differential shear. The bending effect due to the eccentric load path is not considered. The adhesive shear stress distribution τ is given by:

$$\tau = \frac{P\omega}{2b}\cdot\frac{\cosh(\omega x)}{\sinh\left(\frac{\omega l}{2}\right)} + \left(\frac{t_t - t_b}{t_t + t_b}\right)\cdot\left(\frac{\omega l}{2}\right)\cdot\frac{\sinh(\omega x)}{\cosh\left(\frac{\omega l}{2}\right)} \tag{1}$$

where

$$\omega = \sqrt{\frac{G_a}{E t_t t_a}\left(1 + \frac{t_t}{t_b}\right)}$$

The reciprocal of ω has units of length and is the characteristic shear-lag distance, a measure of how quickly the load is transferred from one adherend to the other. t_t is the top adherend thickness, t_b is the bottom adherend thickness, t_a is the adhesive thickness, b is the bonded area width, l is the bonded area length, E is the adherend modulus, G_a is the adhesive shear modulus and P is the force applied to the inner adherend. The origin of x is the middle of the overlap and is shown in Figure 1.

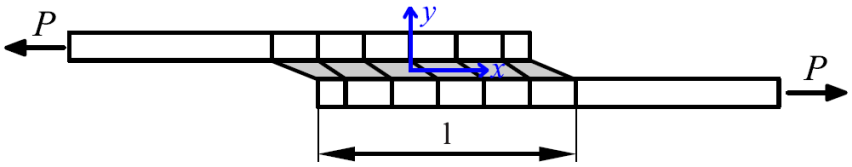

Figure 1: Volkersen model

2.2 Goland & Reissner

Goland & Reissner (1944) were the first to consider the effects due to rotation of the adherends, Figure 2. They divided the problem into two parts: (a) determination of the loads at the edges of the joints, using the finite deflection theory of cylindrically bent plates and (b) determination of joints stresses due to the applied loads.

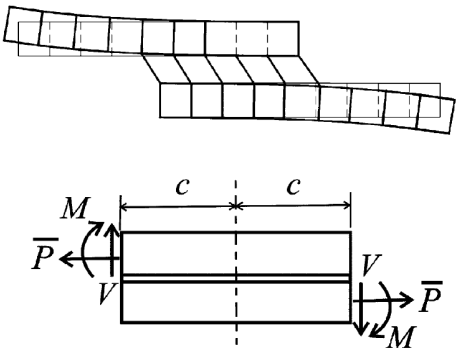

Figure 2: Goland & Reissner model

The adhesive shear stress distribution τ found by Goland & Reissner is given by:

$$\tau = -\frac{1}{8}\frac{\overline{P}}{c}\left\{\frac{\beta c}{t}(1+3k)\frac{\cosh\left(\frac{\beta c}{t}\frac{x}{c}\right)}{\sinh(\beta c/t)}+3(1-k)\right\} \tag{2}$$

where, $\overline{P}$ is the applied tensile load per unit width, c is half of the overlap length, t is the adherend thickness and k is the bending moment factor given by (Goland & Reissner, 1944):

$$k = \frac{\cosh(u_2 c)}{\cosh(u_2 c)+2\sqrt{2}\sinh(u_2 c)}$$

where $u_2 = \sqrt{\frac{3(1-\nu^2)}{2}}\frac{1}{t}\sqrt{\frac{\overline{P}}{tE}}$; $\beta^2 = 8\frac{G_a}{E}\frac{t}{t_a}$ and ν is Poisson's ratio.

The adhesive peel stress distribution σ is given by:

$$\sigma = \frac{1}{\Delta}\frac{\overline{P}t}{c^2}\left[\left(R_2\lambda^2\frac{k}{2}+\lambda k'\cosh(\lambda)\cos(\lambda)\right)\cosh\left(\frac{\lambda x}{c}\right)\cos\left(\frac{\lambda x}{c}\right)\right.$$
$$\left.+\left(R_1\lambda^2\frac{k}{2}+\lambda k'\sinh(\lambda)\sin(\lambda)\right)\sinh\left(\frac{\lambda x}{c}\right)\sin\left(\frac{\lambda x}{c}\right)\right] \tag{3}$$

where k' is the transverse force factor.

$$k' = \frac{kc}{t}\sqrt{3(1-\nu^2)\frac{\overline{P}}{tE}};\ \lambda = \gamma\frac{c}{t};\ \gamma^4 = 6\frac{E_a}{E}\frac{t}{t_a},\ \Delta = \frac{1}{2}(\sin(2\lambda)+\sinh(2\lambda))$$

$$R_1 = \cosh(\lambda)\sin(\lambda) + \sinh(\lambda)\cos(\lambda);\ R_2 = -\cosh(\lambda)\sin(\lambda) + \sinh(\lambda)\cos(\lambda)$$

2.3 Hart-Smith

In contrast with Volkersen or Goland & Reissner, Hart-Smith (1973) considered adhesive plasticity. In their work, they divided the problem in four main steps. First step main goal is obtaining the bending moment M induced at the end of the joint by off-center load. This quantity defines the peak shear and peel stresses in the adhesive. Second step considered the influence of the bending stress on the strength of the adherends. Third step presents the analysis of adhesive shear stress distribution using the elastic-plastic adhesive formulation. Finally, fourth step discusses the problem of peel stresses.

According to Hart-Smith, the adhesive elastic shear stress distribution $\tau_{(x)}$ is given by:

$$\tau_{(x)} = A_2 \cosh(2\lambda' x) + C_2 \tag{4}$$

where,

$$\lambda' = \sqrt{\left[\frac{1+3(1-\nu^2)}{4}\right]\frac{2G_a}{t_a E t}};\ A_2 = \frac{G_a}{t_a E t}\left[\overline{P} + \frac{6(1-\nu^2)M}{t}\right]\frac{1}{2\lambda'\sinh(2\lambda' c)}$$

$$C_2 = \frac{1}{2c}\left[\overline{P} - \frac{A_2}{\lambda'}\sinh(2\lambda' c)\right];\ M = \overline{P}\left(\frac{t+t_a}{2}\right)\frac{1}{1+\xi c+\left(\frac{\xi^2 c^2}{6}\right)};\ \xi^2 = \frac{\overline{P}}{D}$$

and D is the adherend bending stiffness is given by: $D = \dfrac{Et^3}{12(1-\nu^2)}$.

Variables $\overline{P}$, G_a, t_a, E, ν, t, c has the same meaning as presented by Volkersen and Goland & Reissner models. The adhesive peel stress distribution $\sigma_{(x)}$ is given by:

$$\sigma_{(x)} = A\cosh(\chi x)\cos(\chi x) + B\sinh(\chi x)\sin(\chi x) \tag{5}$$

where, $\chi^4 = \dfrac{E_a}{2Dt_a}$; $A = -\dfrac{E_a M[\sin(\chi c) - \cos(\chi c)]}{t_a D\chi^2 e^{(\chi c)}}$; $B = \dfrac{E_a M[\sin(\chi c) + \cos(\chi c)]}{t_a D\chi^2 e^{(\chi c)}}$

and E_a is the Young modulus of the adhesive.

Hart-Smith also considered adhesive shear stress plasticity. The shear stress was modeled using a bi-linear elastic-perfectly plastic approximation. The overlap is divided into three regions, a central elastic region of length d and two outer plastic regions. Coordinates x and x' are defined as shown in Figure 3. Failure of the bonded joint starts as soon as the elastic zone start to plastificate. This take place when τ_p equals to the shear yield strength. This would be the failure criteria considered for the Hart-Smith elastic-plastic model.

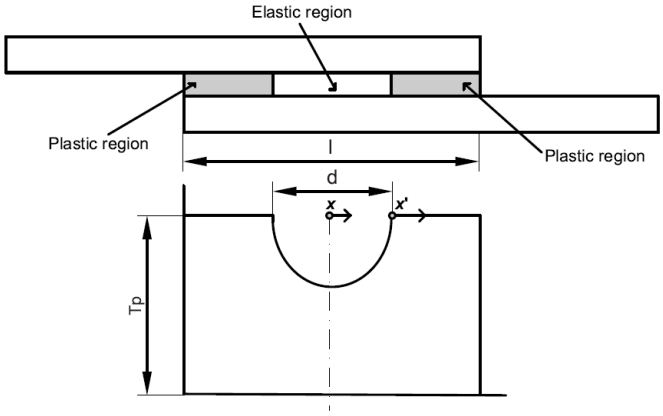

Figure 3: Regions considered by Hart-Smith

The problem is solved in the elastic region in terms of the shear stress according to:

$$\tau_{(x)} = A_2 \cosh\left(2\lambda' x\right) + \tau_p \left(1 - K\right) \tag{6}$$

and the shear strain in the plastic region according to:

$$\gamma_{(x')} = \gamma_e \left\{1 + 2K\left[\left(\lambda' x'\right)^2 + \lambda' x' \tanh\left(\lambda' d\right)\right]\right\} \tag{7}$$

where τ_p is the plastic adhesive shear stress and $A_2 = \dfrac{K\tau_p}{\cosh(\lambda' d)}$.

K and d are solved by an iterative approach using the following equations:

$$\frac{\overline{P}}{l\tau_p}(\lambda' l) = 2\lambda'\left(\frac{l-d}{2}\right) + (1-K)(\lambda' d) + K\tanh(\lambda' d) \tag{8}$$

$$\left[1 + 3k\left(1-\nu^2\right)\left(1+\frac{t_a}{t}\right)\right]\frac{\overline{P}}{\tau_p}\lambda^2\left(\frac{l-d}{2}\right) = 2\left(\frac{\gamma_p}{\gamma_e}\right) + K\left[2\lambda'\left(\frac{l-d}{2}\right)\right]^2 \tag{9}$$

$$2\left(\frac{\gamma_p}{\gamma_e}\right) = K\left\{\left[2\lambda'\left(\frac{l-d}{2}\right) + \tanh(\lambda' d)\right]^2 - \tanh^2(\lambda' d)\right\} \tag{10}$$

where, γ_e and γ_p are the elastic and plastic adhesive shear strain.

2.4 Ojalvo & Eidinoff

Ojalvo & Eidinoff (1978) model is based on Goland & Reissner model. They modified some coefficients in the shear stress equations by adding new terms in the differential equation and considering new boundary conditions for bond peel stress calculation. Their leading work was the first in predicting the variation of shear stress through the bond thickness. The adhesive nondimensional shear stress distribution τ^* found by Ojalvo & Eidinoff is given by:

$$\tau^* = A\cosh\left(\lambda\sqrt{2+6\left(1+\beta\right)^2}\, x^*\right) + B \tag{11}$$

where,

$$A = \frac{2\lambda\left(1+3(1+\beta)^2 k\right)}{\sqrt{2+6(1+\beta)^2}\sinh\left(\lambda\sqrt{2+6(1+\beta)^2}x^*\right)};\ B = 1-\frac{A\sinh\left(\lambda\sqrt{2+6(1+\beta)^2}\right)}{\lambda\sqrt{2+6(1+\beta)^2}}$$

$$\lambda^2 = \frac{G_a c^2}{E^* th};\ \beta = \frac{h}{t}$$

where $E^* = E$ for adherends in plane stress and $E/\left(1-\nu^2\right)$ for adherends in plane strain. G_a, c, E, t are the same variables as defined previously and h is the adhesive thickness. k is the bending moment factor as seen in Hart-Smith model. The maximum nondimensional stress at the bond/adherend interfaces is given by:

$$\tau^{**} = \tau^* \pm \Delta\tau^* \tag{12}$$

where: $\Delta\tau^* = \frac{G_a h}{2E_a}\sigma^{*'}$.

The solution for the nondimensional peel stress σ^* is given by:

$$\sigma^* = C\sinh\left(\alpha_1 x^*\right)\sin\left(\alpha_2 x^*\right) + D\cosh\left(\alpha_1 x^*\right)\cos\left(\alpha_2 x^*\right) \tag{13}$$

where $\alpha_1^2 = \frac{3\beta\lambda^2}{2}+\frac{\rho}{2}$; $\alpha_2^2 = -\frac{3\beta\lambda^2}{2}+\frac{\rho}{2}$ and $\rho^2 = \frac{24E_a c^4}{E^* ht^3}$

Constants *C* and *D* are obtained upon substitution of the derivatives of Eq. (13) into Eqs. (14) and (15)

$$\sigma^{*'''}(\pm 1) - 6\beta\lambda^2\sigma^{*'}(\pm 1) = \mp k\gamma\rho^2(1+\beta) \tag{14}$$

$$\sigma^{*''}(\pm 1) = k\gamma\rho^2(1+\beta) \tag{15}$$

where $\gamma = t/2c$. All analysis was done in a nondimensional basis. Equivalence is given by:

$$\tau^* = \frac{\tau}{\overline{\tau}},\ \sigma^* = \frac{\sigma}{\overline{\tau}},\ x^* = \frac{x}{c},$$

where $\overline{\tau} = \frac{\overline{P}}{2c}$.

3 SOFTWARE IMPLEMENTATIONS

Several analytical methods for the stress distribution calculation in adhesively bonded joints are available in literature. However, implementation and use of analytic models are usually difficult due to its complex non-linear functions of material properties and geometry. This work presents implementation of two softwares. The first one is the implementation of the four models aforementioned the second one is the implementation of the failure criteria for each analytical method. As a consequence, we obtain the failure load for each case and an experimental comparison is finally possible.

3.1 Analytical Methods Analysis

Using the first software we analyzed the four analytical solutions presented. Figure 4 shows the flow diagram of first software. Analysis data are input manually by using a GUI or by reading an internal data base (Figure 5). After defining all the bonded joint required data, an individual analysis is possible, (Figure 6a). The software not only features individual analysis for each analytical model, but also features comparisons between methods, (Figure 6b). Finally, results are shown on the screen as graphics and tables, printing results in a *.txt archive is also possible.

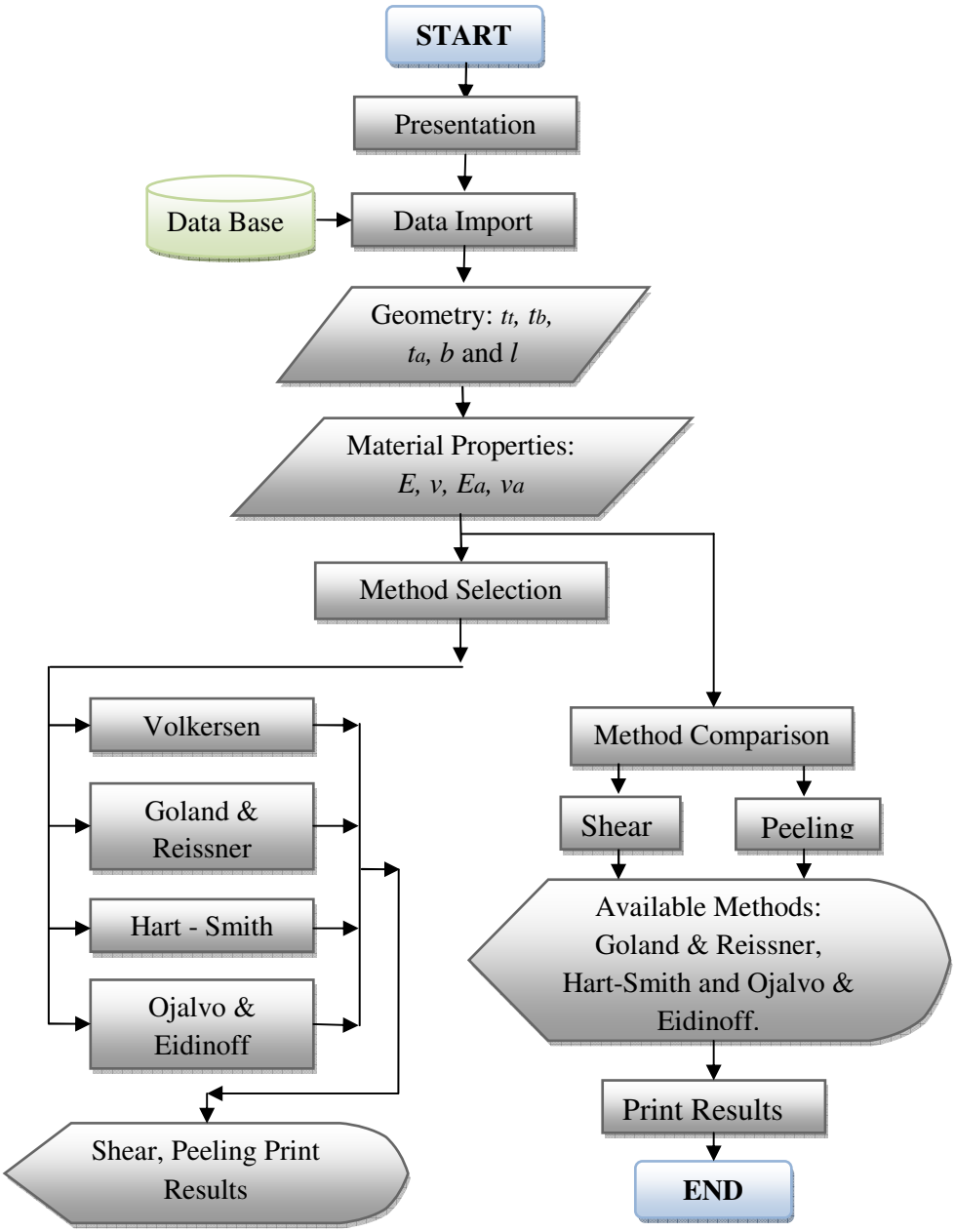

Figure 4: Flow Diagram of first software

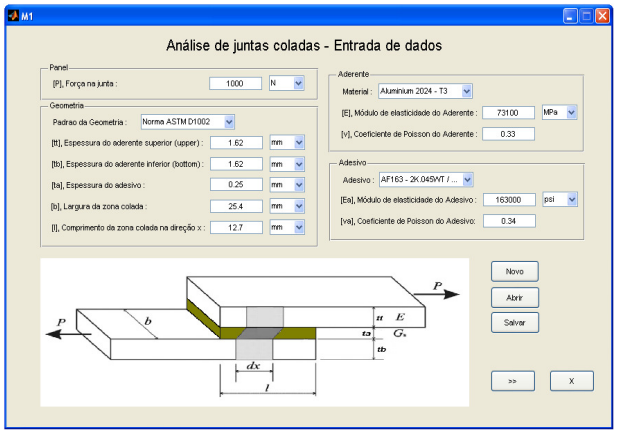

Figure 5: Data input window.

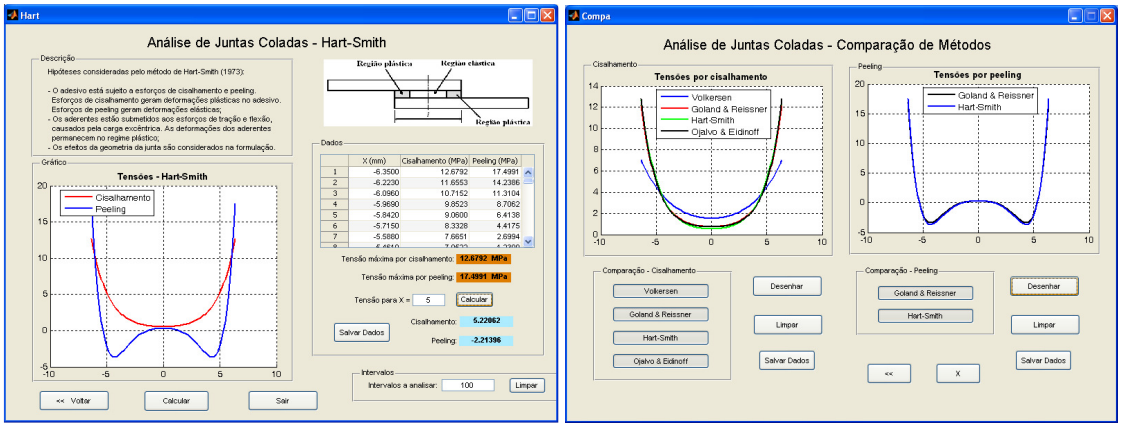

Figure 6: (a) Individual method analysis, (b) Comparison between methods.

3.2 Failure Criteria Analysis

Second software analyzes different failure criteria for each analytical method. Main objective of failure criteria is to obtain a failure load and compare it with the experimental failure load. The flow diagram of this second software is shown in Figure 7.

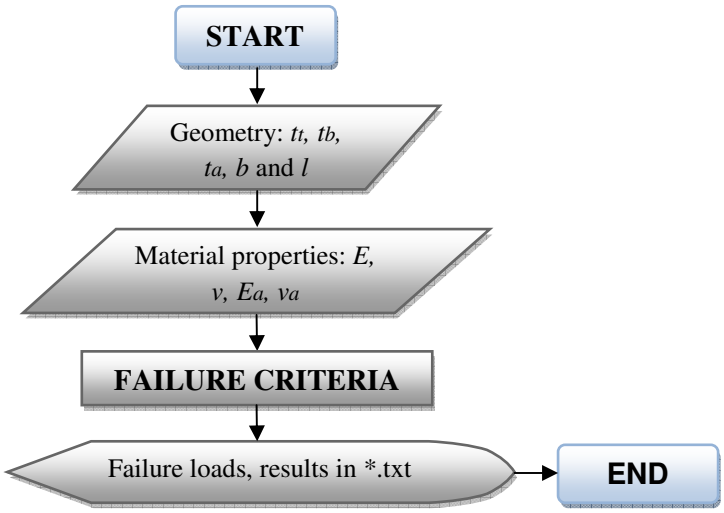

Figure 7: Flow diagram of second software.

4 EXPERIMENTAL VALIDATION

Experimental validation was carried out according to ASTM D1002 standard (Figure 8).

4.1 MATERIALS

The adhesive used was the AF 163-2K.045WT from 3M Company. This adhesive has an ultimate shear strength of 6950 psi, an ultimate peel strength of 7000 psi, a yield strength of 5255 psi and a nominal thickness of 7.5 mils (0.19mm). The adherend used was aluminum 2024-T3, which have an elasticity modulus of 73.1 GPa and a Poisson ratio of 0.33.

4.2 TEST SPECIMENS

Form and dimensions of test specimens are shown in Figure 8. The recommended thickness of adherends is $1.62 \pm 0.125mm$. The recommended length of overlap is $12.7 \pm 0.125mm$. The test speed was 1.30 mm/min.

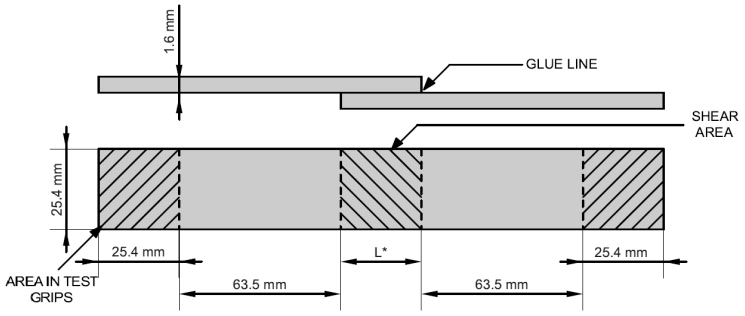

Figure 8: Form and dimensions of test specimens

4.3 TEST RESULTS

For the experimental validation were tested 6 specimens in accordance with the ASTM D1002 standard. For comparisons we considered the mean value of the six specimens tested. The mean failure load was 11284N.

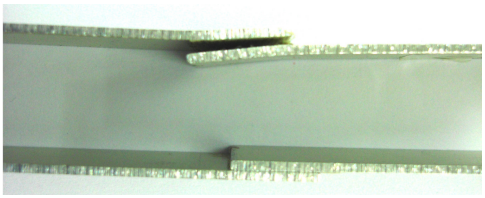

Figure 9: Test specimen before and after testing – junction details.

5 ANALYTICAL COMPARISON

Analytical methods implemented in the software were validated with experimental results. Failure criteria can be seen in Table 1 (Da Silva et al., 2009, c; Rodriguez et al., 2010). For each implemented model was obtained a failure load, then this value was compared with the ultimate load found experimentally, Figure 10.

Analytical Method	Type of analysis	Failure Criterion
Volkersen	Elastic analysis	$\tau > \tau_a$
Goland & Reissner	Elastic analysis	$\tau > \tau_a$ or $\sigma > \sigma_a$
Hart–Smith	Elastic analysis	$\tau > \tau_a$ or $\sigma > \sigma_a$
Hart–Smith	Elasto-plastic analysis	$\tau > \tau_{YS}$
Ojalvo & Eidinoff	Elastic analysis	$\tau > \tau_a$ or $\sigma > \sigma_a$

Table 1: Failure Criterion of each analytical method.

in Table 1, τ_a is the shear strength of the adhesive, σ_a is the peel strength of the adhesive and τ_{YS} is the shear yield strength of the adhesive

Note: As seen in the Hart-Smith elastic-plastic model, failure will start when the elastic zone start to plastificate.

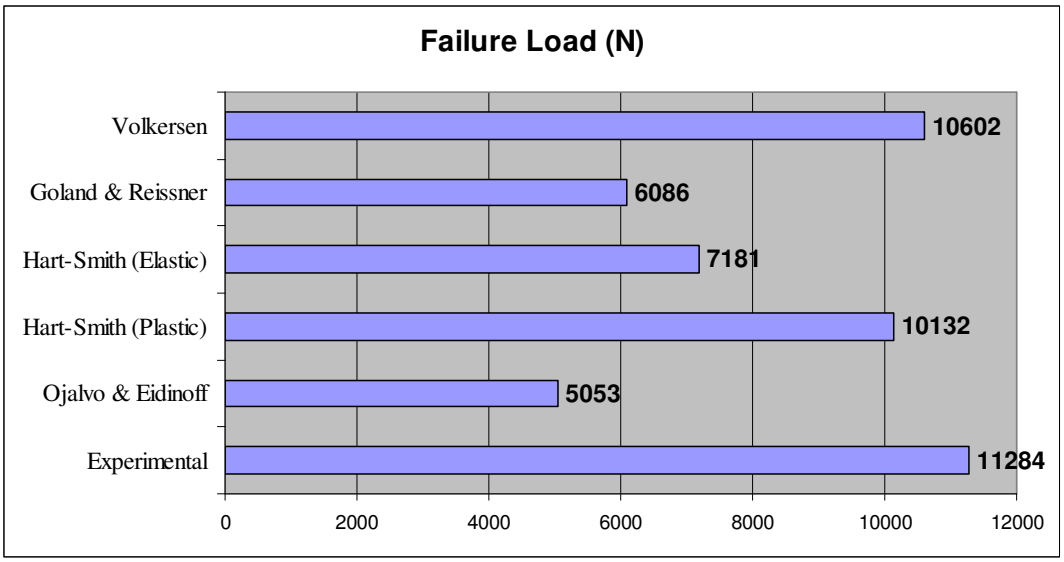

Figure 10: Failure loads of each implemented analytical method.

6 NUMERICAL COMPARISON

Using the first software we can obtain stress distributions for each analytical method. We used geometry and material properties as seen in Sections 4.1 and 4.2. For the numerical validation we used the commercial software ABAQUS®. Were analyzed two types of 3D elements: The linear eight node brick element C3D8 and the quadratic twenty node brick element C3D20. Minimum and maximum values for each case, including analytical results, are shown in Table 2. Figure 11 shows the analytical distribution of Goland & Reissner and Figure 12 shows the Abaqus model used for the numerical comparison. Figure 13 shows comparison among implemented analytical methods results and numerical results for shear stress. Similarly, Figure 14 shows comparison between analytical and numerical results for peel stress.

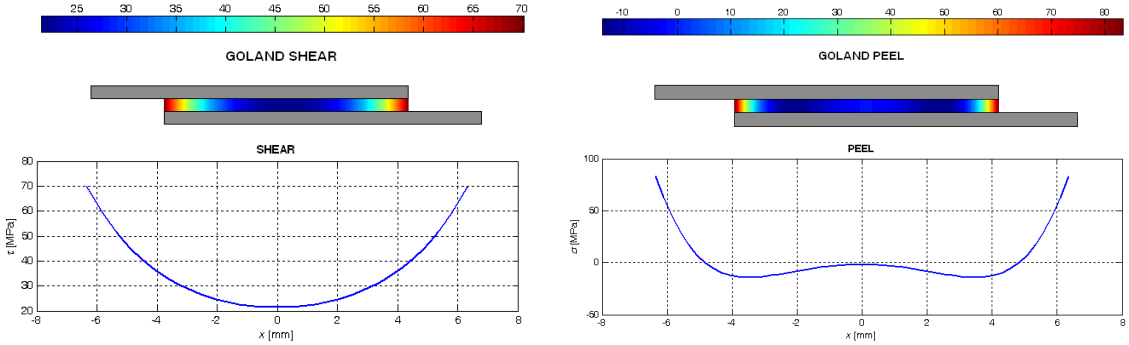

Figure 11: Shear and Peel distributions calculated by Goland & Reissner analytical model

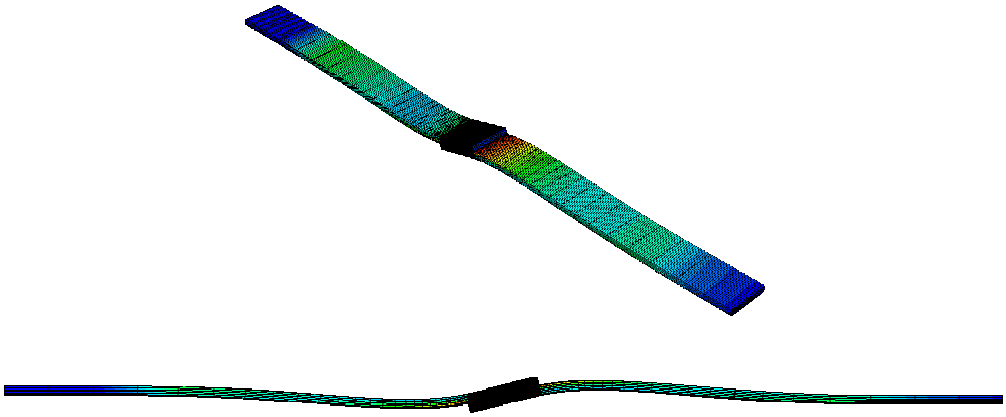

Figure 12: Abaqus mesh of the bonded joint

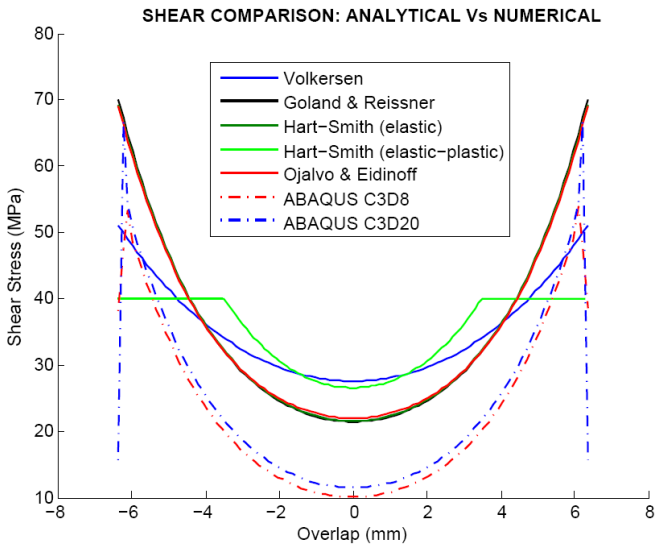

Figure 13: Shear comparison between analytical models and numerical results

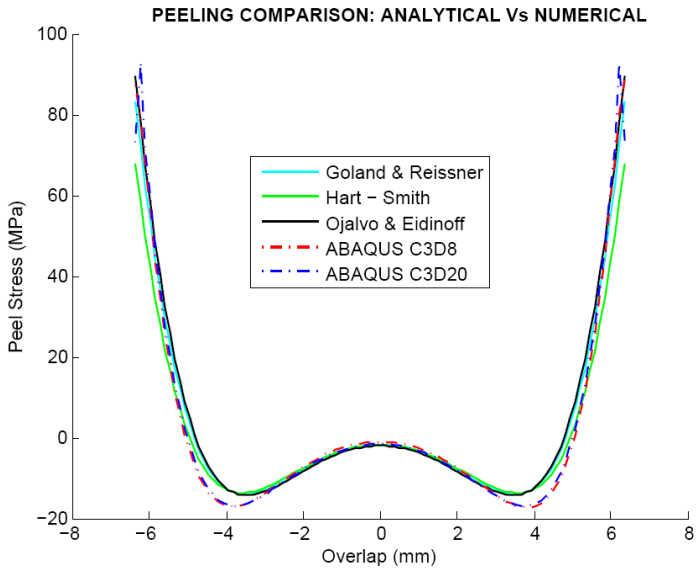

Figure 14: Peeling comparison between analytical models and numerical results

METHOD	Shear (MPa)		Peeling (MPa)	
	Minimum	Maximum	Minimum	Maximum
Volkersen	*27.55*	*50.96*	---	---
Goland & Reissner	*21.43*	*70.10*	*-14.09*	*83.34*
Hart-Smith (elástico)	*21.52*	*69.21*	*-13.75*	*67.91*
Hart-Smith (elasto-plástico)	*26.55*	*40.06*	---	---
Ojalvo & Eidinoff	*21.96*	*69.14*	*-14.34*	*89.63*
ABAQUS C3D8	***10.06***	***53.88***	***-17.32***	***88.48***
ABAQUS C3D20	***11.48***	***66.79***	***-16.96***	***92.98***

Table 2: Minimum and maximum stress values.

7 CONCLUSIONS

There exist many analytical methods available in literature for bonded joint analysis. However, in this paper were implemented only four analytical methods. Methods implemented were considered sufficient to achieve a consistent result, which would be useful for preliminary design purposes and as a consequence would reduce costly tests.

This paper presented a Matlab® implementation of four analytic solutions in a user-friendly software, which features not only individual analysis of each stress distribution, but also a suitable failure criterion and the possibility of comparisons among different methods.

For the validation of the analytical methods implemented were used experimental data in accordance with the ASTM D1002 standard and numerical results obtained by ABAQUS®.

The method whose failure load best approximated to the experimental failure load was the Hart-Smith elastic-plastic model and the method which best approximated to numerical

results was the Ojalvo & Eidinoff model. As a result, the best combination of methods for bonded joint analysis would be Hart Smith elastic-plastic model for shear and Ojalvo & Eidinoff for peeling.

8 REFERENCES

ASTM D1002, "Standard Test Method for Apparent Shear Strength of Single-Lap-Joint Adhesively Bonded Metal Specimens by Tension Loading (Metal-to-Metal)"

Da Silva et al., "Analytical models of adhesively bonded joints – Part I: Literature Survey", *International Journal of Adhesion and Adhesives*, 29, 2009, pp. 319:330

Da Silva et al., "Analytical models of adhesively bonded joints – Part II: Comparative study", *International Journal of Adhesion and Adhesives*, 29, 2009, pp. 331:341

Goland M., Reissner E., "The Stresses in Cemented Joints", *Journal of Applied Mechanics*, Vol.11, March 1944, pp. A17-A27.

Hart-Smith, L. J., "Adhesive-Bonded Single-Lap Joints", NASA CR-112236, January 1973.

Ojalvo I.U, Eidinoff H.L., "Bond Thickness Effects upon Stresses in Single-Lap Adhesive Joints", *American Institute of Aeronautics and Astronautics Journal*, 1978, Vol.16, No 3, pp. 204:211.

Rodríguez, R.Q, Souza, C.O., Sollero, P., Albuquerque, E.L., Rodrigues, M.R.B., "Implementation of failure criteria of adhesively bonded joints", *III International Conference on Welding and Joining of Materials, August 2010.*

Silva L.F.M., Lima R.F.T., Teixeira R.M.S., "Development of a Computer Program for the Design of Adhesive Joints", *The Journal of Adhesion*, 85, 2009, pp. 889:918

Vokersen O., "Nietkraftverteiligung in zugbeanspruchten nietverbindungen mit konstanten Laschenquerschnitten", Luftfahrtforschung, 1938, pp. 15:41.